American Mineralogist, Volume 89, pages 447–454, 2004

Structural and chemical response to varying [4]B content in zoned Fe-bearing olenite from Koralpe, Austria

JOHN M. HUGHES,[1,*] ANDREAS ERTL,[2] M. DARBY DYAR,[3] EDWARD S. GREW,[4] MICHAEL WIEDEN-BECK,[5] AND FRANZ BRANDSTÄTTER[6]

[1]Department of Geology, Miami University, Oxford, Ohio 45056, U.S.A.
[2]Institut für Mineralogie und Kristallographie, Geozentrum, Universität Wien, Althanstrasse 14, A-1090 Wien, Austria
[3]Department of Geography and Geology, Mount Holyoke College, South Hadley, Massachusetts 01075, U.S.A.
[4]Department of Geological Sciences, University of Maine, Orono, Maine 04469-5711, U.S.A.
[5]GeoForschungszentrum Potsdam, Telegrafenberg, Potsdam, D-14473, Germany
[6]Mineralogisch-Petrographische Abteilung, Naturhistorisches Museum, Burgring 7, A-1014 Wien, Austria

ABSTRACT

Tourmaline has recently been shown to incorporate large amounts of substituent B at the tetrahedral site. To characterize the response of the tourmaline atomic arrangement to differing amounts of substitution of B for Si, five samples were separated from a core-to-rim (~3 mm) section of an Fe-bearing olenite with a dark green core and a nearly colorless rim from Koralpe, Austria. Crystal structures of the five samples were refined to *R* values <0.018 using three-dimensional X-ray methods, and the compositions of the crystals were determined by electron microprobe, secondary ion mass spectrometric, and Mössbauer analyses. From core to rim, [4]B increases monotonically from 0.35 to 0.65 apfu, whereas the mean T-O distance decreases from 1.621 to 1.610 Å. Optimized formulae using chemical and structural data range from $^{X}(Na_{0.632}Ca_{0.145}\square_{0.223})\ ^{Y}(Al_{1.320}Fe^{2+}_{1.202}Li_{0.190}Mg_{0.086}Ti_{0.028}Mn^{2+}_{0.024}\square_{0.150})\ ^{Z}Al_{6.00}\ B_{3.00}\ ^{T}(Si_{5.525}B_{0.333}Al_{0.130}Be_{0.012})\ O_{27}\ [(OH)_{3.19}O_{0.81}]$ (core composition) to $^{X}(Na_{0.408}Ca_{0.290}K_{0.002}\square_{0.300})\ ^{Y}(Al_{2.338}Li_{0.365}Fe^{2+}_{0.084}Mn^{2+}_{0.009}Mg_{0.005}Ti_{0.005}\square_{0.194})\ ^{Z}Al_{6.00}\ B_{3.00}\ ^{T}(Si_{4.989}B_{0.615}Al_{0.362}Be_{0.034})\ O_{27}\ [(OH)_{3.41}O_{0.59}]$ (rim composition). The variation of chemistry and structure, coupled with short-range order constraints, demonstrates that (1) the average tetrahedral bond length (<T-O>) reflects the substitution of [4]B, (2) tourmaline samples with relatively high Fe^{2+} contents (ca. 1 apfu Fe^{2+}) and <T-O> distances up to 1.621 Å can contain significant amounts of [4]B (up to ca. 0.3 apfu), (3) the presence of substantial [4]B is limited to, or more common in Al-rich tourmalines, (4) the presence of [4]B substituents favors OH at the O3 site, (5) the presence of Ca or Na at the X site is not simply correlated with occupancy of [4]B in the adjacent tetrahedral ring, and (6) no two B-substituted tetrahedra will link through bridging O atoms.

INTRODUCTION

Most crystal structure studies are undertaken on a single crystal extracted from a rock or a larger crystal. Such studies provide a single "snapshot" of the atomic arrangement and its chemistry, but do not provide information regarding changes in the atomic arrangement with changes in chemistry. In this study we extracted five single crystals at 800 μm intervals from a zoned single crystal of excess-boron olenite tourmaline, and characterize the chemistry and crystal structure of each of the extracted crystals. Such a study provides, in contrast to the single "snapshot," a "movie" that elucidates the covariance of structure and chemistry that occurs in portions of a single crystal of magmatic origin or one that may have crystallized from supercritical fluid (Kalt et al. 2001). Similar "movies" based on chemical analyses alone do give some information on this covariance (e.g., for schorl-B excess olenite, Kalt et al. 2001), but the added crystal-structure refinements provide a much better documentation of the site occupancies.

Until recently, it was commonly accepted that tourmaline did not contain boron as a substituent at the T (tetrahedral) site. However, Ertl et al. (1997) discovered an olenite (Al-rich tourmaline) that contained approximately one [4]B atom per six T sites (by refinement and chemical analysis), and Hughes et al. (2000) offered a more detailed analysis that confirmed all aspects of the original work. The latter authors proffered a high-quality crystal structure, electron- and ion-probe analyses, and a summary of the structural responses to the incorporation of large amounts of substituent [4]B. Marler and Ertl (2002) found 0.8 ± 0.2 apfu [4]B in this colorless olenite by ^{11}B magic-angle-spinning nuclear magnetic resonance spectroscopy, which is in good agreement with the values obtained by structure refinement. Olenite from the type locality (Kola Peninsula, Russia) also contains substantial [4]B (Schreyer et al. 2002). Wodara and Schreyer (1997, 1998, 2001), Schreyer et al. (2000), and Marler et al. (2002) described synthetic Al-rich tourmalines with even more extensive substitution of B at the T site: up to 2.2 [4]B. These discoveries imply that the assumption of ideal boron stoichiometry is not valid for the more widespread elbaite-schorl-rossmanite tourmalines, but instead boron content must be measured.

In this work we extracted five crystals from core to rim of a larger single tourmaline crystal from a small pegmatite near the Stoffhütte, Koralpe, Styria, Austria (Postl and Moser 1987;

* E-mail: hughesjm@muohio.edu

Ertl and Brandstätter 1998). This pegmatite was the source of colorless [4]B-rich olenite described by Ertl et al. (1997) and Hughes et al. (2000), and of the solid solution between magnesian schorl and excess-boron olenite characterized chemically by Kalt et al. (2001). In contrast to the latter, our crystal was not taken from the pegmatite contact with mylonitic garnet-biotite schists, but from the center of the pegmatite. Preliminary EMPA of the original uncut, nearly colorless to dark green Fe-bearing olenite crystal showed extensive zoning from core to rim in Si, implying zoning in [4]B. After the individual single crystals were cut from the larger single crystal, the five samples were ground to spheres for crystal structure analysis (T1-T5, from rim to core, Fig. 1). After mounting, these structure crystals were then submitted for electron and ion microprobe analyses; Mössbauer analysis was made of additional crystals extracted from sample T3. The final electron microprobe analyses (EMPA) are in good agreement with the preliminary EMPA results. The combination of crystal-structure analysis and chemical analysis yields information regarding the change in atomic arrangement with changes in chemistry in excess-boron tourmalines.

Experimental methods

Crystal structure

Five crystals were cut from a 4 mm, core-to-rim section of the single crystal, and were subsequently ground to spheres (approximately 300 µm diameter, Fig. 1) for the single-crystal X-ray studies. Data were collected with a Bruker Platform goniometer equipped with an APEX 4K CCD detector and Mo$K\alpha$ radiation, to 65° 2θ. Data were integrated using the Bruker program SAINT, and absorption was corrected using the program SADABS. Least-squares refinement was undertaken using the Bruker program SHELXTL version 6.10, utilizing neutral-atom scattering factors and corrections for anomalous dispersion. The refinements were routine; the X site was modeled with Na scattering factors and released multiplicity, and the Y site was similarly modeled using Al scattering factors. The Z site was also modeled using Al scattering factors but with fixed occupancy of $Al_{1.00}$, because a released multiplicity showed this site to be essentially fully occupied by Al. The T site was modeled with B and Si scattering factors, with the assumption that B + Si = 1.

Table 1 contains crystal data and results of the structure refinement for samples T1 (rim) through T5 (core) extracted from the larger single crystal, and Table 2 contains atomic parameters for the five structure crystals; Table 3 reports tetrahedral bond lengths for the five tourmaline structures.

Chemical analysis

Subsequent to structure determination, the samples were prepared for EMPA and ion microprobe or secondary ion mass spectrometric analysis (SIMS). The quasi-spherical samples were embedded in epoxy on a single 2.5 cm diameter round glass slide and were then sectioned by polishing. Both backscattered-electron and cathode-luminescence SEM images were used to check overall homogeneity and for better targeting the SIMS primary ion beam.

EMPA were conducted at Rutgers University using a JEOL JXA-8600 microprobe operating at 20 kV accelerating voltage, a beam current of 20 nA, and a beam size of 1 µm on the carbon-coated crystals. Twenty-second counting times were used for all analyzed elements. Reported analyses are the average of two analyses for each sample.

We used a Cameca ims 6f ion microprobe at GeoForschungszentrum Potsdam, Germany to determine the absolute concentration of Li, Be, and B in the samples. Hydrogen concentrations were not measured but taken from Kalt et al. (2001). The carbon-coated glass slide was cleaned in high-purity ethanol for 5 minutes in an ultrasonic bath and then dried in an oven at ~50 °C for 20 min prior to depositing a 30 nm thick gold coat directly on the carbon coated sample. The operating conditions for SIMS analyses were nominal 12.5 kV accelerating potential in order to generate a 2 nA $^{16}O^-$ primary beam that was focused to a ~6 µm diameter spot on the sample surface. A nominal secondary extraction voltage of +10 kV was employed, to which a 60 V energy offset was applied in conjunction with a 75 V

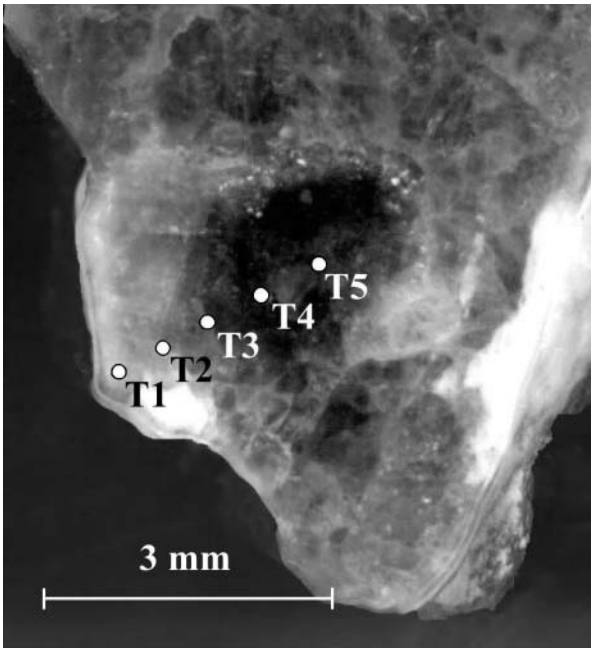

Figure 1. Crystal of [4]B-rich Fe-bearing olenite from Koralpe, Austria. Points T1-T5 denote approximate locations of crystals extracted for crystal structure analysis and electron- and ion-probe analysis. Total distance from T1-T5 is approximately 3 mm.

Table 1a. Crystal data and details of structure refinements for Fe-bearing to Fe-rich olenite from the Koralpe, Styria, Austria

Sample	*a* (Å)	*c* (Å)	*V* (Å³)	Reflections in cell refinement
T1	15.7537(4)	7.0707(2)	1519.72(12)	5864
T2	15.7713(4)	7.0760(2)	1524.25(12)	5854
T3	15.7959(4)	7.0815(2)	1530.20(12)	5885
T4	15.8472(4)	7.0988(2)	1543.90(12)	5903
T5	15.9013(4)	7.1213(2)	1559.40(12)	5911

Notes: Crystal size = approximately 300 µm spheres, space group *R3m*, frame width 0.20°, scan time 10 s, 4800 frames, detector distance 5 cm, absorption correction by SADABS.

Table 1b. Crystal data and details of structure refinements for Fe-bearing to Fe-rich olenite from the Koralpe, Styria, Austria

Sample	Redundancy	Unique Data	Refined Parms.	$R1_{(I > 4\sigma I)}$	GooF	Δρ peaks (e–/Å³)
T1	9.57	1335	94	0.0147	1.187	+0.34, –0.32
T2	17.32	1340	94	0.0137	1.139	+0.21, –0.27
T3	9.54	1342	94	0.0148	1.173	+0.28, –0.34
T4	9.52	1346	94	0.0160	1.119	+0.36, –0.30
T5	9.53	1373	94	0.0176	1.065	+0.34, –0.23

Notes: Crystal size = approximately 300 µm spheres, space group *R3m*, frame width 0.20°, scan time 10 s, 4800 frames, detector distance 5 cm, absorption correction by SADABS.

TABLE 2. Atomic parameters and equivalent isotropic *U* values for atoms in olenite from the Koralpe, Styria, Austria

Atom	Crystal	*x*	*y*	*z*	U_{eq}	Occ.
Na	T1	0	0	1/4	0.0158(3)	$Na_{0.91(1)}$
	T2	0	0	1/4	0.0170(3)	$Na_{0.92(1)}$
	T3	0	0	3/4	0.0170(4)	$Na_{0.94(1)}$
	T4	0	0	1/4	0.0178(4)	$Na_{0.99(1)}$
	T5	0	0	1/4	0.0196(6)	$Na_{0.90(1)}$
AlY	T1	0.12149(3)	0.06074	–0.32526(18)	0.0097(1)	$Al_{0.874(3)}$
	T2	0.12143(3)	0.06071	–0.32815(18)	0.0096(1)	$Al_{0.906(2)}$
	T3	0.87871(3)	0.93935	0.32912(18)	0.0099(1)	$Al_{0.968(2)}$
	T4	0.12142(3)	0.06071	–0.33189(20)	0.0098(1)	$Al_{1.094(2)}$
	T5	0.12204(3)	0.06102	–0.33702(28)	0.0099(1)	$Al_{1.286(4)}$
AlZ	T1	0.29671(2)	0.26049(2)	–0.35784(16)	0.00898(7)	$Al_{1.00}$
	T2	0.29674(2)	0.26042(2)	–0.35941(16)	0.00881(7)	$Al_{1.00}$
	T3	0.70312(2)	0.73953(2)	0.35947(17)	0.00886(8)	$Al_{1.00}$
	T4	0.29709(2)	0.26061(3)	–0.36039(19)	0.00870(9)	$Al_{1.00}$
	T5	0.29753(3)	0.26084(3)	–0.36206(28)	0.00843(9)	$Al_{1.00}$
T	T1	0.19120(2)	0.18935(2)	0.03544(16)	0.00789(9)	$Si_{0.892(3)}B_{0.108}$
	T2	0.19136(2)	0.18949(2)	0.03338(17)	0.00754(8)	$Si_{0.905(3)}B_{0.095}$
	T3	0.80847(2)	0.81037(2)	0.96712(17)	0.00762(9)	$Si_{0.915(3)}B_{0.085}$
	T4	0.19179(2)	0.18986(2)	0.03137(19)	0.0074(1)	$Si_{0.937(4)}B_{0.063}$
	T5	0.19190(2)	0.18994(3)	0.02874(28)	0.0071(1)	$Si_{0.941(4)}B_{0.059}$
B	T1	0.10908(5)	0.21815	0.48617(23)	0.0085(2)	$B_{1.00}$
	T2	0.10914(5)	0.21828	0.48456(24)	0.0084(2)	$B_{1.00}$
	T3	0.89084(5)	0.78168	0.51582(25)	0.0088(2)	$B_{1.00}$
	T4	0.10938(6)	0.21876	0.48285(29)	0.0090(3)	$B_{1.00}$
	T5	0.10971(8)	0.21943	0.48112(39)	0.0097(3)	$B_{1.00}$
O1	T1	0	0	–0.1925(3)	0.0159(3)	$O_{1.00}$
	T2	0	0	–0.1938(3)	0.0180(3)	$O_{1.00}$
	T3	0	0	0.1927(3)	0.0210(4)	$O_{1.00}$
	T4	0	0	–0.1930(4)	0.0257(5)	$O_{1.00}$
	T5	0	0	–0.1936(5)	0.0325(8)	$O_{1.00}$
O2	T1	0.05986(3)	0.11972	0.5246(2)	0.0150(2)	$O_{1.00}$
	T2	0.06000(4)	0.12000	0.5217(2)	0.0161(2)	$O_{1.00}$
	T3	0.93984(4)	0.87969	0.4796(2)	0.0170(2)	$O_{1.00}$
	T4	0.06044(5)	0.12088	0.5170(3)	0.0184(3)	$O_{1.00}$
	T5	0.06093(6)	0.12185	0.5137(4)	0.0194(3)	$O_{1.00}$
O3	T1	0.25944(8)	0.12972	–0.4586(2)	0.0135(2)	$O_{1.00}$
	T2	0.26057(8)	0.13029	–0.4602(2)	0.0141(2)	$O_{1.00}$
	T3	0.73834(9)	0.86917	1.4604(2)	0.0145(2)	$O_{1.00}$
	T4	0.2634(1)	0.13169	–0.4615(3)	0.0145(2)	$O_{1.00}$
	T5	0.2653(1)	0.13262	–0.4628(3)	0.0153(3)	$O_{1.00}$
O4	T1	0.09389(4)	0.18777	0.1101(2)	0.0141(2)	$O_{1.00}$
	T2	0.09384(4)	0.18767	0.1077(2)	0.0136(2)	$O_{1.00}$
	T3	0.90624(4)	0.81248	0.8933(2)	0.0137(2)	$O_{1.00}$
	T4	0.09357(5)	0.18715	0.1045(3)	0.0135(2)	$O_{1.00}$
	T5	0.09344(6)	0.18688	0.1002(3)	0.0139(3)	$O_{1.00}$
O5	T1	0.18588(8)	0.09294	0.1309(2)	0.0147(2)	$O_{1.00}$
	T2	0.18598(8)	0.09299	0.1287(2)	0.0141(2)	$O_{1.00}$
	T3	0.81398(9)	0.90699	0.8719(2)	0.0143(2)	$O_{1.00}$
	T4	0.1862(1)	0.09310	0.1264(3)	0.0142(2)	$O_{1.00}$
	T5	0.1867(1)	0.09335	0.1224(3)	0.0139(3)	$O_{1.00}$
O6	T1	0.19343(4)	0.18312(5)	–0.1910(2)	0.0099(1)	$O_{1.00}$
	T2	0.19389(4)	0.18359(5)	–0.1930(2)	0.0100(1)	$O_{1.00}$
	T3	0.80548(5)	0.81585(5)	0.1934(2)	0.0105(1)	$O_{1.00}$
	T4	0.19538(6)	0.18497(6)	–0.1950(2)	0.0108(2)	$O_{1.00}$
	T5	0.19643(7)	0.18609(8)	–0.1969(3)	0.0115(2)	$O_{1.00}$
O7	T1	0.28650(5)	0.28584(4)	0.1102(2)	0.0100(1)	$O_{1.00}$
	T2	0.28653(5)	0.28595(4)	0.1089(2)	0.0098(1)	$O_{1.00}$
	T3	0.71346(5)	0.71399(5)	0.8910(2)	0.0101(1)	$O_{1.00}$
	T4	0.28663(6)	0.28622(6)	0.1084(2)	0.0101(1)	$O_{1.00}$
	T5	0.28616(7)	0.28613(7)	0.1067(3)	0.0107(2)	$O_{1.00}$
O8	T1	0.20935(5)	0.26996(5)	0.4710(2)	0.0098(1)	$O_{1.00}$
	T2	0.20938(5)	0.27000(5)	0.4696(2)	0.0098(1)	$O_{1.00}$
	T3	0.79066(5)	0.72996(5)	0.5304(2)	0.0102(1)	$O_{1.00}$
	T4	0.20935(6)	0.27011(6)	0.4685(2)	0.0106(2)	$O_{1.00}$
	T5	0.20954(7)	0.27039(8)	0.4672(3)	0.0117(2)	$O_{1.00}$
H3	T1	0.252(3)	0.126	0.400(7)	0.08(1)	$H_{1.00}$
	T2	0.256(3)	0.128	0.411(6)	0.07(1)	$H_{1.00}$
	T3	0.742(3)	0.871	0.591(6)	0.06(1)	$H_{1.00}$
	T4	0.262(3)	0.131	0.416(6)	0.05(1)	$H_{1.00}$
	T5	0.263(3)	0.132	0.420(6)	0.04(1)	$H_{1.00}$

TABLE 3. Tetrahedral interatomic distances (Å) in Fe-bearing to Fe-rich olenite from the Koralpe, Styria, Austria

T1		T2	
T1-O7	1.6007(7)	T-O7	1.6030(7)
T1-O6	1.6053(7)	T-O6	1.6061(7)
T1-O4	1.6098(4)	T-O4	1.6122(4)
T1-O5	1.6254(5)	T-O5	1.6276(5)
Mean	1.6103	Mean	1.6122
T3		T4	
T3-O7	1.6050(7)	T-O7	1.6107(8)
T3-O6	1.6067(8)	T-O6	1.6110(9)
T3-O4	1.6150(4)	T-O4	1.6207(5)
T3-O5	1.6307(5)	T-O5	1.6365(6)
Mean	1.6144	Mean	1.6197
T5			
T5-O6	1.6108(11)		
T5-O7	1.6132(10)		
T5-O4	1.6237(6)		
T5-O5	1.6382(7)		
Mean	1.6215		

energy bandpass. The mass spectrometer was operated at a moderately high mass resolving power of $M/\delta M$ = 1800, which is sufficient to resolve all significant isobaric interferences from the mass spectrum. A 750 µm diameter field aperture was employed, which corresponded to a 60 µm diameter field of view. The primary ion beam was centered on the axis of the field aperture prior to each analysis. Each analysis employed an unrastered five minute pre-burn that locally removed the conductive gold film and also established equilibrium sputtering conditions. A single measurement consisted of 12 cycles of the peak stepping sequence: 6.9 background (0.1s), ^{7}Li (2s), ^{9}Be (10s), ^{11}B (2s), and ^{30}Si (2s). The measurement, including the five minute preburn, thus lasted slightly over 9 minutes. The relative sensitivity factors for the three light elements were defined using the dravite sample no. 108796 described by Dyar et al. (2001). In total there were $N = 9$ measurements obtained from the dravite reference sample and these a mean external precision of 10.5% for Li, 2.9% for Be, and 0.5% for B. Table 4 contains the results of the chemical analyses.

Mössbauer analysis

Because the sample size was extremely small, we were only able to obtain Mössbauer results for on a single sample. From the T3 region of the original single crystal, 80 mg of tourmaline was extracted for Mössbauer analysis. The sample was prepared by crushing and then mixing the sample with sucrose under acetone before placing it in a sample holder confined by cello tape. The resultant sample thickness was 1.27 mg Fe/cm^2, well below the thin-absorber thickness approximation of Long et al. (1983) but sufficient for acquisition of a useful spectrum.

A room-Temperature Mössbauer spectrum was acquired to determine Fe^{2+} and Fe^{3+} content in the Mineral Spectroscopy Laboratory at Mount Holyoke College. A 20 mCi ^{57}Co in Rh source was used in a WEB Research Co. spectrometer. Collection time was two days. Results were calibrated against an α-Fe foil of 6 µm thickness and 99% purity. The detection limit for Fe^{3+} in this sample is estimated at ±2–3%.

The spectrum was fit using the WMOSS software of WEB Research Co., an implementation of the Voigt-based fitting method developed by Rancourt and Ping (1991). This method has been shown to be most appropriate for samples in which the Fe atoms do not have homogeneous environments, but rather have different types of nearest-neighbor and next-nearest-neighbor environments. This is certainly the case in the complicated tourmaline structure. Fits with up to four quadrupole splitting distributions were obtained.

RESULTS AND DISCUSSION

As noted previously, examination of the atomic arrangement and the chemical composition of a series of crystals extracted from a larger, zoned single-crystal provides unique information regarding the covariance of structure and composition. Several observations can be made about the covariance of structural and chemical parameters in the Koralpe olenite. Using quadratic programming methods, Wright et al. (2000) offered a method of optimizing the occupants of cation sites in minerals with multiply occupied cation sites; the optimized formula essentially minimizes the differences between the formula obtained from the results of the chemical analysis and that obtained by single crystal structure refinement (SREF). Using that method

with the structure refinement and chemical data obtained in this study, the structural formulae of these tourmaline samples are (T5 = core, T1 = rim):

T5: $^{X}(Na_{0.632}Ca_{0.145}\square_{0.223})\ ^{Y}(Al_{1.320}Fe^{2+}_{1.202}Li_{0.190}Mg_{0.086}Ti_{0.028}Mn^{2+}_{0.024}\square_{0.150})\ ^{Z}Al_{6.00}\ B_{3.00}\ ^{T}(Si_{5.525}B_{0.333}Al_{0.130}Be_{0.012})\ O_{27}\ [(OH)_{3.19}O_{0.81}]$,

T4: $^{X}(Na_{0.545}Ca_{0.245}\square_{0.240})\ ^{Y}(Al_{1.792}Fe^{2+}_{0.669}Li_{0.226}Mg_{0.038}Mn^{2+}_{0.022}Ti_{0.013}\square_{0.240})\ ^{Z}Al_{6.00}\ B_{3.00}\ ^{T}(Si_{5.354}B_{0.353}Al_{0.270}Be_{0.023})\ O_{27}\ [(OH)_{3.25}O_{0.75}]$,

T3: $^{X}(Na_{0.478}Ca_{0.252}\square_{0.270})\ ^{Y}(Al_{2.116}Fe^{2+}_{0.336}Li_{0.272}Mn^{2+}_{0.015}Mg_{0.011}Ti_{0.010}\square_{0.240})\ ^{Z}Al_{6.00}\ B_{3.00}\ ^{T}(Si_{5.242}B_{0.482}Al_{0.249}Be_{0.027})\ O_{27}\ [(OH)_{3.31}O_{0.69}]$,

T2: $^{X}(Na_{0.480}Ca_{0.241}\square_{0.300})\ ^{Y}(Al_{2.222}Li_{0.342}Fe^{2+}_{0.190}Mg_{0.010}Ti_{0.009}Mn^{2+}_{0.007}\square_{0.220})\ ^{Z}Al_{6.00}\ B_{3.00}\ ^{T}(Si_{5.132}B_{0.542}Al_{0.295}Be_{0.031})\ O_{27}\ [(OH)_{3.32}O_{0.68}]$,

T1: $^{X}(Na_{0.408}Ca_{0.290}K_{0.002}\square_{0.300})\ ^{Y}(Al_{2.338}Li_{0.365}Fe^{2+}_{0.084}Mn^{2+}_{0.009}Mg_{0.005}Ti_{0.005}\square_{0.194})\ ^{Z}Al_{6.00}\ B_{3.00}\ ^{T}(Si_{4.989}B_{0.615}Al_{0.362}Be_{0.034})\ O_{27}\ [(OH)_{3.41}O_{0.59}]$.

The optimized formula for a colorless, nearly Fe-free boron-rich olenite from the same locality was given by Hughes et al. (2000) as $^{X}(Na_{0.400}Ca_{0.294}\square_{0.306})\ ^{Y}(Al_{2.424}Li_{0.357}\square_{0.219})\ ^{Z}(Al_{5.916}\square_{0.084})\ B_{3.00}\ ^{T}(Si_{4.854}B_{1.062}Al_{0.084})\ O_{27}\ [F_{0.06}(OH)_{3.31}O_{0.63}]$, and the optimized formula for Al-rich schorl, also from the same locality, was given by Ertl and Hughes (2002) as $^{X}(Na_{0.64}Ca_{0.10}K_{0.06}\square_{0.20})\ ^{Y}(Fe^{2+}_{1.72}Al_{1.08}Ti_{0.11}Zn_{0.03}\square_{0.06})\ ^{Z}(Al_{5.70}Mg_{0.20}Fe^{2+}_{0.08}Mn_{0.02})\ B_{3.00}\ ^{T}(Si_{5.76}B_{0.24})\ O_{27}\ [F_{0.11}(OH)_{3.31}O_{0.58}]$. It is clearly evident that the [4]B content increases concomitantly with the Al content at the Y site, a relationship verified for the studied tourmaline sample. This relationship is probably valid for many Al-rich tourmalines, but not for those in which the Fe^{3+} content of the Y site is high. Fe^{2+} rich tourmaline samples at this locality with formulae similar to samples T4 and T5 might not contain much more [4]B than Al-rich because the short range order requires essentially Al_3 at the Y site (Hughes et al. 2000; Schreyer et al. 2002) to incorporate B at the T site.

Ertl et al. (2002) found a strong correlation (r = –0.985) between the bond-angle distortion of the Z octahedron and <Y-O> for tourmaline samples which contain 3 (OH) at the V site (O3 site). The crystal structures of zoned olenite from this paper give additional information on this correlation by filling the gap for tourmaline with <Y-O> bond lengths in the range 1.957–1.995 Å. Including the new structural data the r-value for this correlation improves to r = –0.991.

SiO_2 content

Analysis of B by microbeam methods is difficult and analytical errors are invariably high, and, not surprisingly, attempts to confirm the existence of tetrahedral boron in tourmaline by microanalysis of B were not definitive. The analytical errors typically were larger than the amount of B in excess of the putative 3.00 apfu B occupying the trigonal site. Although the tourmalines detailed herein contain substantial excess B, certainly enough to distinguish despite the relatively large errors inherent in boron analyses, we have found that an effective way to determine the presence of excess B by chemical analysis is by the chemical analysis of Si.

Possible tetrahedral occupants of tourmaline are Si, Al, B, Fe^{3+} (Dyar et al. 1998), and Be (0.09 wt% BeO is the maximum reported in tourmaline, cf. Kalt et al. 2001 and Grew 2002), but only Si, Al, and B have been found in significant amounts. The presence of significant Al but little B is evidenced in increased <T-O> bond distances (Hawthorne 1996); absent such increased tetrahedral bond lengths and without evidence of [4]Fe, we can assume that B + Si + Al = 6, as tetrahedral vacancies would render the structure unstable. Figure 2 displays the variation of wt% SiO_2 from the chemical analysis and the refined [4]B from the independently determined crystal-structure analysis. The covariance (r = –0.99) illustrates the concomitant decrease in SiO_2 content that occurs with incorporation of substituent [4]B and suggests that both chemical analysis for silica and crystal structure analysis for tetrahedral site-scattering are effective methods of estimating the amount of substituent [4]B. Figure 2 could be used as a rough calibration curve to estimate [4]B from SiO_2 content measured by EMPA in low-Fe and very low-Mg tourmaline from samples of this locality when a structure refinement is not available.

Tetrahedral bond lengths

Ertl et al. (2001) have shown that tetrahedral bond lengths respond to substituent boron and aluminum, but not as in the hard-sphere model. Figure 3 depicts the decrease in <T-O> bond length with the addition of substituent B at the tetrahedral site. The monotonic decrease in mean tetrahedral bond length with increasing substituent [4]B is also seen in individual bond lengths,

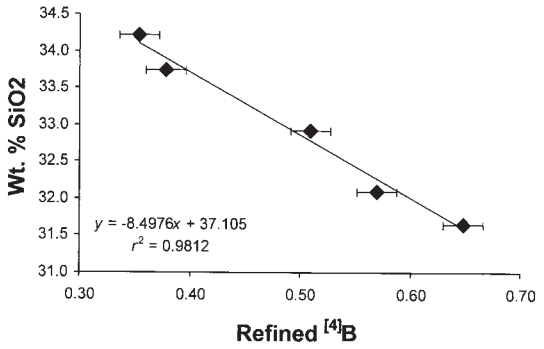

FIGURE 2. Variation of analyzed SiO_2 vs. refined [4]B. Error bars enclose 1 sigma.

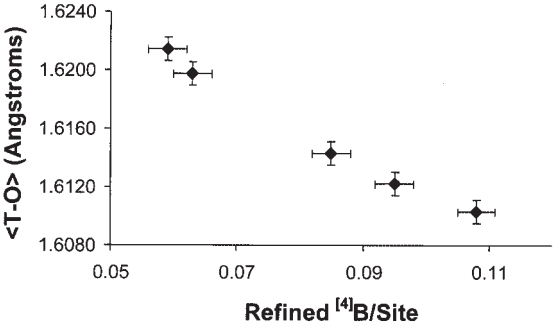

FIGURE 3. Variation of <*T*-O> with refined [4]B. Error bars enclose 1 sigma.

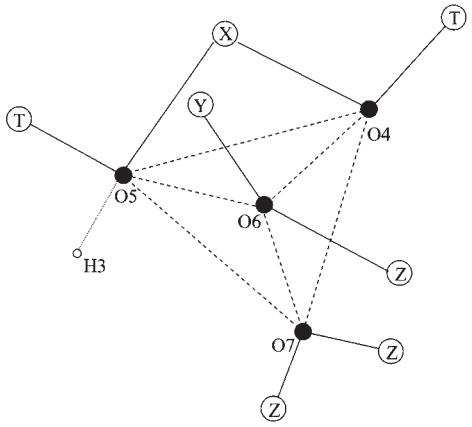

FIGURE 4. Depiction of coordination of tetrahedral O atoms in tourmaline. N.B. O6 is directly above the T site at the center of the tetrahedron so the T-O6 bond is covered.

which are not plotted. The greatest range in bond length is seen in the T-O4 bond (0.014 Å), which is not surprising given that O4 is only bonded to X in addition to T (Fig. 4). Because occupancy of X appears to play a subordinate role in T occupancy (see below), O4 must satisfy its bond valence largely through shortening its bonds to the two neighboring tetrahedral occupants.

[6]Al content

All tourmaline samples that have been found to contain B above 3.00 apfu, both synthetic and natural, have been aluminous, containing nearly $Al_{9.00}$ at the octahedral sites (the major occupant at those sites, other than Al, is Li). Figure 5 illustrates the monotonic increase of [4]B with increasing analyzed Al_2O_3; an inflection point corresponds to a dramatic decrease of Fe at the octahedral sites.

The substitution of B and Al for Si at the tetrahedral sites yields decreased bond valence to the coordinating O atoms. The Pauling bond-valence of an Si-O bond is 1.0 valence units (v.u.), vs. 0.75 v.u. for a B-O or Al-O bond. Such a diminution of bonding to the coordinating O atoms can be mitigated by the presence of trivalent atoms (e.g., Al) at the Y and Z octahedral sites.

Figure 4 depicts the coordination of the tetrahedral O atoms in tourmaline. A trivalent substituent at the Y or Z site will provide 0.50 v.u. Pauling bond valence to the coordinating O atoms, vs. 0.33 v.u. for a divalent substituent. As shown in Figure 4, trivalent substituents such as Al at Y and Z would contribute 0.34 v.u. more to O6 and O7 than such sites occupied by divalent octahedral cations, the additional bond valence being more than sufficient to cover the loss of bonding from the substituent [4]B or [4]Al; substituent Li at those sites offsets a portion of the charge balance achieved by replacing Fe^{2+} with Al. As shown in Figure 5, Al_2O_3 increases with increasing [4]B, suggesting Al plays a major role in charge balance. It can also be suggested that substituent Al at Z would, in addition to providing the additional balancing charge, cause a reduction in size in the Z-edge-sharing octahedral cluster to accommodate the reduction in size of the B-substituted tetrahedral rings.

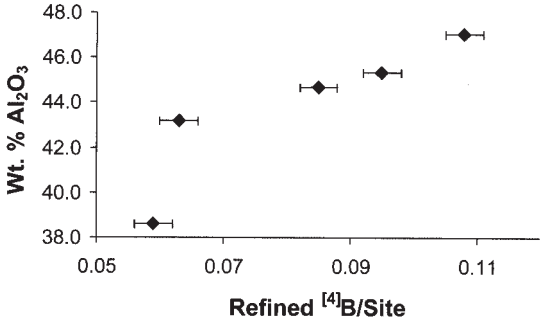

FIGURE 5. Variation of analyzed Al_2O_3 with refined [4]B. Error bars enclose 1 sigma.

O3 occupant

Bond-valence maintenance of the tetrahedral O atoms is a critical factor in the substitution of B at the tetrahedral sites. The bridging O atom O5 gains a small amount of hydrogen bonding (typically ca. 0.05 v.u.) from the hydrogen atom associated with O3 (= H3). To alleviate the loss of bonding from the [4]B substituent, we can suggest that the presence of [4]B substituents favors OH at the O3 site. In each of the refinements of T1-T5, a hydrogen atom at the site associated with O3 was easily located, suggesting the O3 site is occupied by hydroxyl in [4]B substituted tourmaline. In all the samples F was sought but not detected.

X-site occupants

Hawthorne (1996) evaluated the substitutions that facilitate incorporation of trivalent substituents in the tourmaline tetrahedral sites. Because bridging O atoms O4 and O5 receive bond valence from the occupant of the X site (typically □, Na, Ca), the bond-valence lost to the bridging O atoms from incorporation of $[4]B^{3+}$ can be mitigated by incorporation of Ca in the X site. Hughes et al. (2000) showed that in Koralpe olenite, Ca or Na at the adjacent X site contribute 0.12 or 0.08 valence units (vu), respectively, to the adjacent O4 anion, and 0.15 or 0.10, respectively, to the adjacent O5 atom. It is thus tempting to suggest that local ordering would demand a Ca atom, or minimally an Na atom, at the X site adjacent to a tetrahedral ring with substituent [4]B. Indeed, Foit et al. (1989) demonstrated that a coupling exists between [4]Al and X-site charge in Ben Lomond tourmalines.

In an analysis of short-range order in the Koralpe olenite, if it is assumed that there are three [4]B in a tetrahedral ring (there is no reason to predict that occupation, as this model is only conjecture), there is not enough Ca to occupy the X site adjacent to the ring, and some of the X sites must be occupied by Na (Hughes et al. 2000). Furthermore, in that olenite, if it is assumed that there is no more than one substituent [4]B per tetrahedral ring, many of the substituted tetrahedra must exist adjacent to vacant X sites. In synthesis experiments, W. Schreyer and colleagues have synthesized Al-rich tourmalines (olenite) with even greater amounts of substituent [4]B than found in natural samples, and Al-rich tourmaline samples which have a vacancy-dominant X site (Schreyer et al. 2000; Wodara and Schreyer 1997, 1998, 2001; Marler et al. 2002). It thus is evident (counter intuitively), par-

TABLE 4. Chemical analyses of Fe-bearing to Fe-rich olenite from the Koralpe, Austria

	T1	T1*	T2	T2*	T3	T3*	T4	T4*	T5	T5*
SiO_2	31.65	31.84	32.10	32.62	32.92	33.07	33.74	33.32	34.21	33.83
TiO_2	0.04	0.04	0.07	0.08	0.08	0.08	0.11	0.11	0.22	0.23
B_2O_3	13.35†	13.37	12.83†	13.04	12.68†	12.73	12.26†	12.09	11.77†	11.83
Al_2O_3	47.09	47.11	45.37	45.93	44.70	44.77	43.19	42.57	38.63	38.71
BeO	0.09	0.09	0.08	0.08	0.07	0.07	0.06	0.06	0.03	0.03
FeO	0.64	0.64	1.42	1.45	2.52	2.53	4.80	4.98	8.92	8.80
MnO*	0.07	0.07	0.05	0.05	0.11	0.11	0.16	0.16	0.17	0.17
MgO	0.02	0.02	0.04	0.04	0.05	0.05	0.16	0.16	0.35	0.35
CaO	1.72	1.55	1.52	1.43	1.55	1.48	1.36	1.42	0.73	0.83
Li_2O	0.57	0.58	0.53	0.54	0.42	0.43	0.33	0.35	0.28	0.29
Na_2O	1.34	1.42	1.46	1.57	1.44	1.55	1.61	1.75	1.84	2.00
K_2O	0.01	0.01	0.00	–	0.00	–	0.00	–	0.00	–
H_2O	3.25‡	3.26	3.11§	3.17	3.11§	3.13	2.91‖	3.03	2.91‖	2.93
Total sum	99.84	100.00	98.58	100.00	99.65	100.00	100.69	100.00	100.06	100.00
T site (apfu)										
Si	4.977	4.989	5.137	5.132	5.246	5.242	5.357	5.354	5.630	5.525
[4]B	0.623	0.615	0.544	0.542	0.488	0.482	0.360	0.353	0.344	0.333
[4]Al	0.366	0.362	0.288	0.295	0.239	0.249	0.260	0.270	0.014	0.130
Be	0.034	0.034	0.031	0.031	0.027	0.027	0.023	0.023	0.012	0.012
Sum T site	6.000	6.000	6.000	6.000	6.000	6.000	6.000	6.000	6.000	6.000
[3]B	3.000	3.000	3.000	3.000	3.000	3.000	3.000	3.000	3.000	3.000
Y, Z site										
Al	8.361	8.338	8.269	8.222	8.156	8.116	7.822	7.792	7.477	7.320
Li	0.361	0.365	0.341	0.342	0.269	0.272	0.211	0.226	0.185	0.190
Fe^{2+}	0.084	0.084	0.190	0.190	0.336	0.336	0.637	0.669	1.228	1.202
Mn^{2+}	0.009	0.009	0.007	0.007	0.015	0.015	0.022	0.022	0.024	0.024
Mg	0.005	0.005	0.010	0.010	0.011	0.011	0.038	0.038	0.086	0.086
Ti	0.005	0.005	0.009	0.009	0.010	0.010	0.013	0.013	0.028	0.028
Sum Y, Z site	8.825	8.806	8.826	8.780	8.797	8.760	8.743	8.760	9.028	8.850
X site										
Na	0.408	0.430	0.453	0.480	0.445	0.478	0.496	0.545	0.587	0.632
Ca	0.290	0.260	0.261	0.241	0.264	0.252	0.232	0.245	0.129	0.145
K	0.002	0.002	–	–	–	–	–	–	–	–
Sum X site	0.700	0.692	0.714	0.721	0.709	0.730	0.728	0.790	0.716	0.777
Sum cations	18.525	18.498	18.540	18.501	18.506	18.490	18.471	18.550	18.744	18.627
H	3.409	3.409	3.320	3.320	3.306	3.306	3.082	3.250	3.194	3.194

* Wt% calculated from optimal site-occupancies and normalized to 100%.
† Recalculated from the refinement of the T site (Table 2). The calculated values are within an error of 2–11% in good agreement with the SIMS analyses of B_2O_3.
‡ From Ertl et al. (1997).
§ From Kalt et al. (2001), SIMS value for rim-compositions for olenite from the pegmatite.
‖ From Kalt et al. (2001), SIMS value for Fe-rich olenite with ca. 1 apfu Fe^{2+}. Fluorine is in all samples below the detection limit. Mn has been calculated as Mn^{2+}. A value is not considered significant unless its value exceeds the uncertainty.

ticularly from the definitive synthesis experiments, that despite the charge-balancing valence provided by the X-site occupant it is not necessary to have an adjacent X-site occupant for charge balance in [4]B-substituted tourmaline. Within the tourmaline samples describe herein, there is sufficient Na and Ca at the X sites to occupy the X site adjacent to any [4]B-substituted tetrahedral ring, but there is no linear relationship between substituent [4]B and X-site occupants.

Fe in [4]B-bearing tourmaline

As noted in this study, [4]B appears to be more common in Al-rich tourmalines. To determine the oxidation state of iron in the tourmaline, a Mössbauer spectrum was collected from sample T3. The best fit is shown in Figure 6 and Table 5. Following the established conventions for fits using quadrupole splitting distribution, γ, which is the Lorentzian full peak-width and half-maximum intensity, was constrained to be 0.20 mm/s, which is roughly the natural linewidth of Fe. The ratio of Lorentzian heights of the two lines in an elemental quadrupole doublet, h_+/h_-, was constrained for all components to be equal to zero. The values for δ_0 (the value of isomer shift, δ, when the distributed hyperfine parameter has a value of zero) and δ_1 (the coupling of δ to the distributed hyperfine parameter) were constrained to be the same (but allowed to vary as a group) for all sub-components based upon the assumption that these all represent Fe^{2+} atoms

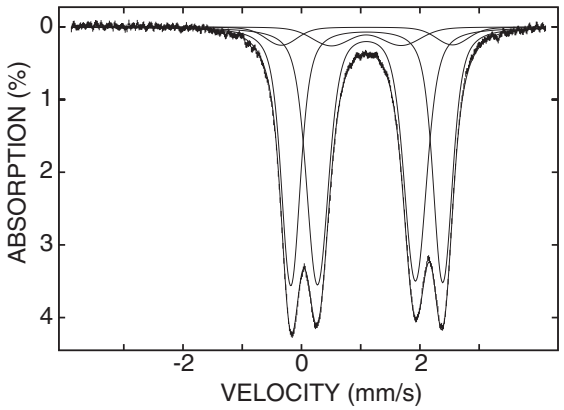

FIGURE 6. Mössbauer spectrum for sample T3.

at the Y site. The remaining parameters, including the center of the Gaussian component of the Δ-distribution (Δ_0), the width of the quadrupole splitting distribution (δ_Δ), and the relative area of the doublets (A), were allowed to vary freely. Isomer shift (δ) is calculated using $\delta = \delta_1 * \Delta_0 + \delta_0$. Details relating to the application of these parameters can be found in Rancourt and Ping (1991).

The parameters of the four modeled Gaussian sub-components (Table 5) all correspond to Fe^{2+} at the Y site, in keeping with the assignments proposed by Pieczka et al. (1997) and used by Dyar et al. (1998). With varying combinations of constraints for the parameters of each sub-component, there was no evidence for any contribution from Fe^{3+} in either tetrahedral or octahedral coordination. Similarly, we attempted fits using three vs. four subcomponents. The total quadrupole-splitting distribution was very similar for both the three sub-component fits and the four sub-component fits, and it is well-defined, independent of the number of Gaussian sub-components used. This result is typical of the Voigt-based/QSD fitting method used here, which yields results that are quite stable.

TABLE 5. Mössbauer parameters for tourmaline

	Doublet no. 1	Doublet no. 2	Doublet no. 3	Doublet no. 4
Δ_0	2.89	2.57	1.65	1.19
δ_Δ	1.06	0.52	0.65	1.32
δ_0	1.09	1.09	1.09	1.09
δ_1	0.01	0.01	0.01	0.01
δ	1.10	1.10	1.10	1.09
A	0.05	0.42	0.48	0.06

Notes: Results are given in mm/s relative to the center point of a Fe foil calibration spectrum. γ, , which is the Lorentzian full peak width and half maximum intensity, was constrained to be 0.20 mm/s, which is the natural linewidth of Fe. Δ_0 = the center of a Gaussian component of the Δ-distribution. δ_Δ = the width of the quadrupole splitting distribution. δ_0 = the value of isomer shift, δ, when the distributed hyperfine parameter has a value of zero. δ_1 = the coupling of δ to the distributed hyperfine parameter. $\delta = \delta_1 * \Delta_0 + \delta_0$. *A* = the relative area of doublet. h_+/h_- = the ratio of Lorentzian heights of the two lines in an elemental quadrupole doublet, was constrained for all components to be equal to zero. Details can be found in Rancourt and Ping (1991). The reduced X^2 value for this fit was 0.60.

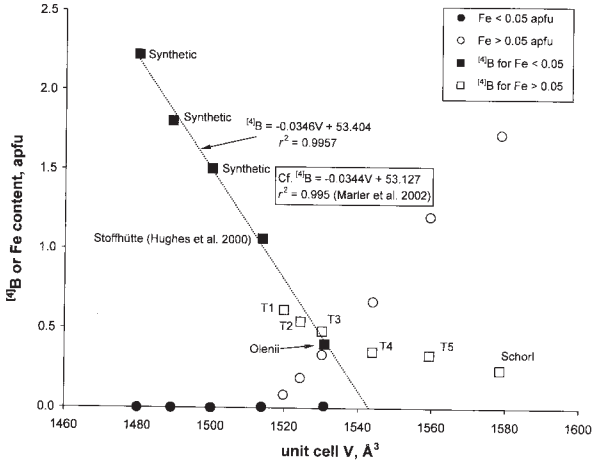

FIGURE 7. Relationship between unit-cell volume and [4]B and Fe content in [4]B-bearing tourmalines.

However, because the X^2 value was dramatically lower for the four sub-component fit (0.60 vs. 1.25 for the three sub-component fit), we have chosen that fit for Figure 6 and Table 5. No matter which fit was used, there was no evidence for Fe^{3+} at any site.

Unit-cell volume

The unit-cell volume of tourmaline responds to both incorporation of [4]B and Fe with antithetic effects. Figure 7 depicts the variation of unit-cell volume with both substituents. As seen therein, [4]B-bearing tourmalines that contain essentially no Fe exhibit a linear correlation between unit-cell volume and [4]B content. However, as Fe enters the tourmaline atomic arrangement in amounts greater than 0.05 apfu, the diminution of cell volume with incorporation of [4]B is mitigated by the substituent Fe.

[4]B-[4]B avoidance

Like Al-Al avoidance in feldspars, a similar maxim can be erected for [4]B-bearing tourmaline. If two adjacent tetrahedral sites contain substituent B, the intervening O atoms (O4, O5) would each receive only 1.5 v.u. bonding from the adjacent tetrahedral sites. Additional bonding from the X-site occupant as well as that received (by O5) from hydrogen bonding is not sufficient to satisfy the bonding at the O sites. We can suggest that no two adjacent tetrahedra are occupied by B (or Al) substituents.

Formula calculation

Our results, together with those reported by Schreyer et al. (2002) for olenite from the type locality and Stoffhütte, as well as studies of synthetic olenite, show that calculating a formula assuming $B_{3.00}$ apfu can be problematic for Al-rich tourmalines. If excess B exists as [4]B, such a calculation will yield an Si value (apfu) that is too high, which leaves the false impression that [4]B and [4]Al are absent. If the sum of all oxides (including calculated B_2O_3, H_2O, Li_2O) is much lower than 100%, the presence of [4]B should be suspected. Another error is overestimating H_2O content. The assumption that (OH + F) = 4.00 is valid only for Li-rich and some Li-bearing tourmalines (elbaite, liddicoatite, Li-bearing olenite from the type locality, Li-bearing schorl; Dyar et al. 1998; Schreyer et al. 2002).

ACKNOWLEDGMENTS

This paper is dedicated to Walter Postl, who orignially discovered the pegmatite from which the samples were collected; his keen observations set the stage for continuing work on minerals from the pegmatite. The structure portion of this work was supported by NSF grants EAR-9627222, EAR-9804768, and EAR-0003201 (all to J.M.H.). We thank M. vanGemeren for his careful preparation of the five single crystals in the EMPA mount and J. Delaney of Rutgers University for the electron microprobe analyses of the five crystals. N. Foit and Y. Fuchs kindly provided perceptive and constructive reviews. W. Lack of the Miami University Instrumentation Laboratory is thanked for efficiently maintaining all the X-ray equipment.

REFERENCES CITED

Dyar, M.D., Taylor, M.E., Lutz, T.M., Francis, C.A., Guidotti, C.V., and Wise, M. (1998) Inclusive chemical characterization of tourmaline: Mössbauer study of Fe valence and site occupancy. American Mineralogist, 83, 848–864.

Dyar, M.D., Wiedenbeck, M., Robertson, D., Cross, L.R., Delaney, J.S., Ferguson, K., Francis, C.A., Grew, E.S., Guidotti, C.V., Hervig, R.L., Hughes, J.M., Husler, J., Leeman, W., McGuire, A.V., Rhede, D., Rothe, H., Paul, R.L., Richards, I., J.D., and Yates, M. (2001) Reference minerals for the microanalysis of light elements. Geostandards Newsletter, 25, 441–463.

Ertl, A. and Brandstätter, F. (1998) Olenit mit Borüberschuß aus einem Metapegmatit östlich der Stoffhütte, Koralpe, Steiermark, Österreich. Mitteilungen der Abteilung für Mineralogie am Landesmuseum Joanneum, 62/63, 3–21.

Ertl, A. and Hughes, J.M. (2002) The crystal structure of an aluminum-rich schorl overgrown by boron-rich olenite from Koralpe, Styria, Austria. Mineralogy and Petrology, 75, 69–78.

Ertl, A., Pertlik, F., and Bernhardt, H.-J. (1997) Investigations on olenite with excess boron from the Koralpe, Styria, Austria. Österreichische Akademie der Wissenschaften, Mathematisch-naturwissenschaftliche Klasse, Anzeiger Abt. 1, 134, 3–10.

Ertl, A., Hughes, J.M., and Marler, B. (2001) Empirical formulae for the calculation of <*T*-*O*> and *X*–O2 bond lengths in tourmaline and relations to tetrahedrally coordinated boron. Neues Jahrbuch für Mineralogie Monatshefte, 2001(12), 548–557.

Ertl, A., Hughes, J.M., Pertlik, F., Foit, F.F. Jr., Wright, S.E., Brandstätter, F., and Marler, B. (2002) Polyhedron distortions in tourmaline. Canadian Mineralogist, 40, 153–162.

Foit, F.F. Jr., Fuchs, Y., and Myers, P.E. (1989) Chemistry of alkali-deficient schorls from two tourmaline-dumortierite deposits. American Mineralogist, 74, 1317–1324.

Grew, E.S. (2002) Beryllium in metamorphic environments (emphasis on aluminous compositions). In E.S. Grew, Ed., Beryllium: Mineralogy, Petrology, and Geochemistry. Reviews in Mineralogy and Geochemistry, 50, 487–549. Mineralogical Society of America, Washington, D.C.

Hawthorne, F.C. (1996) Structural mechanisms for light-element variations in tourmaline. Canadian Mineralogist, 34, 123–132.

Hughes, J.M., Ertl, A., Dyar, M.D., Grew, E., Shearer, C.K., Yates, M.G., and Giudotti, C.V. (2000) Tetrahedrally coordinated boron in a tourmaline: Boron-rich olenite from Stoffhütte, Koralpe, Austria. Canadian Mineralogist, 38, 861–868.

Kalt, A., Schreyer, W., Ludwig, T., Prowatke, S., Bernhardt, H.-J., and Ertl, A. (2001) Complete solid solution between magnesian schorl and lithian excess-boron olenite in a pegmatite from the Koralpe (eastern Alps, Austria). European Journal of Mineralogy, 13, 1191–1205.

Long, G.J., Cranshaw, T.E., and Longworth, G. (1983) The ideal Mössbauer effect absorber thickness. Mössbauer Effect Reference Data Journal, 6, 42–49.

Marler, B. and Ertl, A. (2002) Nuclear magnetic resonance and infrared spectroscopic study of excess-boron olenite from Koralpe, Styria, Austria. American Mineralogist, 87, 364–367.

Marler, B., Borowski, M., Wodara, U., and Schreyer, W. (2002) Synthetic tourmaline (olenite) with excess boron replacing silicon in the tetrahedral site: II. Structure analysis. European Journal of Mineralogy, 14, 763–771.

Pieczka, A., Kraczka, J., and Zabinski, W. (1997) Mössbauer spectra of Fe^{3+}-poor schorls: reinterpretation of the spectra on a basis of an ordered structure model. Abstract to Tourmaline 1997 International Symposium on Tourmaline, Nové Mesto na Morave, Czech Republic, p. 74–75.

Postl, W. and Moser, B. (1987) Ein Turmalinpegmati östlich der Stoffhütte, Koralpe, Steiermark. Mitteilungen der Abteilung für Mineralogie am Landesmuseum Joanneum, 55, 13–20,

Rancourt, D.G. and Ping, J.Y. (1991) Voigt-based methods for arbitrary-shape static hyperfine parameter distributions in Mössbauer spectroscopy. Nuclear Instruments and Methods in Physics Research, B58, 85–97.

Schreyer, W., Wodara, U., Marler, B., van Aken, P.A., Seifert, F., and Robert, J.L. (2000) Synthetic tourmaline (olenite) with excess boron replacing silicon in the tetrahedral site: I. Synthesis conditions, chemical and spectroscopic evidence. European Journal of Mineralogy, 12, 529–541.

Schreyer, W., Hughes, J.M., Bernhardt, H.-J., Kalt, A., Prowatke, S., and Ertl, A. (2002) Reexamination of olenite from the type locality: detection of boron in tetrahedral coordination. European Journal of Mineralogy, 14, 935–942.

Wodara, U. and Schreyer, W. (1997) Turmaline mit Borüberschuß im System Na_2O-Al_2O_3-B_2O_3-SiO_2-H_2O (NABSH). Berichte der Deutschen Mineralogischen Gesellschaft, Beihefte zum European Journal of Mineralogy, 9, No. 1, 394.

———(1998) Tetrahedral boron in tourmalines of the system Na_2O-Al_2O_3-B_2O_3-SiO_2-H_2O. Terra Nova, 10 (abstract supplement no. 1), 68–69.

———(2001) X-site vacant Al-tourmaline: a new synthetic end-member. European Journal of Mineralogy, 13, 521–532.

Wright, S.E., Foley, J.A., and Hughes, J.M. (2000) Optimization of site-occupancies in minerals using quadratic programming. American Mineralogist, 85, 524–531.

MANUSCRIPT RECEIVED DECEMBER 20, 2002
MANUSCRIPT ACCEPTED SEPTEMBER 21, 2003
MANUSCRIPT HANDLED BY LEE GROAT